

# Structure–Photoluminescence Correlation for Two Crystalline Polymorphs of a Thiophene–Phenylene Co-Oligomer with Bulky Terminal Substituents

Tommaso Nicolini,<sup>†</sup> Antonino Famulari,<sup>†</sup> Teresa Gatti,<sup>†,‡</sup> Javier Martí-Rujas,<sup>‡</sup> Francesca Villafiorita-Monteleone,<sup>§</sup> Eleonora V. Canesi,<sup>‡</sup> Francesco Meinardi,<sup>⊥</sup> Chiara Botta,<sup>§</sup> Emilio Parisini,<sup>‡</sup> Stefano Valdo Meille,<sup>\*,†</sup> and Chiara Bertarelli<sup>\*,†,‡</sup>

<sup>†</sup>Dipartimento di Chimica, Materiali e Ingegneria Chimica, Politecnico di Milano, P.zza L. Da Vinci 32, 20133 Milano, Italy

<sup>‡</sup>Center for Nano Science and Technology@Polimi, Istituto Italiano di Tecnologia, Via Pascoli 70/3, 20133 Milano, Italy

<sup>§</sup>Istituto per lo Studio delle Macromolecole (ISMAC), CNR, Via Bassini 15, 20133 Milano, Italy

<sup>⊥</sup>Dipartimento Scienze dei Materiali, Università degli Studi di Milano Bicocca, Via Cozzi 55, 20125 Milano, Italy

**A**mong organic semiconducting materials, short conjugated oligomers have attracted very broad interest due to their fine-tunable and normally well-defined structural features. Thiophene–phenylene co-oligomers are known for their remarkable optical properties and good charge mobility, which make them suitable candidates for electronics or optoelectronic applications.<sup>1–4</sup> Appropriate side groups on the conjugated backbone allow modulation of electronic properties and improve solubility, paving the way to flexible solution processing.<sup>5</sup> At the same time, maintaining precise control over nanoscale molecular organization in the solid state is crucial as it can strongly affect the physical properties of the material. More specifically, the absorption and emission properties of aromatic compounds in the solid state are usually interpreted with reference to J- and H-aggregate models,<sup>6,7</sup> the former showing generally higher photoluminescence rate constants. For crystalline oligothiophenes<sup>8</sup> and thiophene–phenylene co-oligomers,<sup>9–12</sup> the absorption and emission properties present mainly H-features, implying a nonemissive or weakly emissive 0–0 transition in the photoluminescence spectra,<sup>13</sup> as reported for example for odd-numbered oligothiophenes.<sup>14</sup> However, H-aggregates are enticing because of their stability and intrinsic structural anisotropy, which give easy access to important ASE and lasing effects. Efforts to

obtain highly photoluminescent H-aggregates with oligothiophenes and other aromatic oligomers by the introduction of appropriate substituents<sup>15,16</sup> are hence ongoing.

Bulky substituents may be used to prevent strong aromatic interactions that, in most cases, are assumed to quench light emission. A notable case involves phenylene–vinylene oligomers<sup>17</sup> in which the introduction of methyls in the meta positions of terminal phenylenes preserves H-aggregation in crystals, albeit with loss of the herringbone motif, while enhancing light emission quantum yields (QYs). In the mentioned instance, as in other cases where physical properties are modulated by chemical modifications of molecules, a quantitative assessment of the role of packing and intermolecular interactions is prevented by the differences in molecular structure.

In this respect, the ability of a given molecule to adopt different crystal structures offers a unique opportunity to modulate the material physical properties while allowing for quantitative packing comparisons. Despite its often elusive

**Received:** May 9, 2014

**Accepted:** June 6, 2014

**Published:** June 6, 2014

nature, polymorphism in quaterthiophenes (4T) is not unusual; in some cases, structural variations are minor, as for unsubstituted quaterthiophene, which may adopt two crystal forms with a very similar herringbone packing.<sup>18</sup> In other, less frequent, instances, as for some  $\alpha$ - and  $\beta$ -substituted 4T derivatives, conformational polymorphs with different optoelectronic properties have been found.<sup>19</sup>

Here, we report the case of a 4T derivative (5,5'''-bis(3,5-di-*tert*-butyl-4-methoxyphenyl)-2,2':5',2'':5'',2'''-quaterthiophene (DP-4T))<sup>20</sup> showing two remarkably different, stable polymorphs that can be produced selectively (Figure 1). More

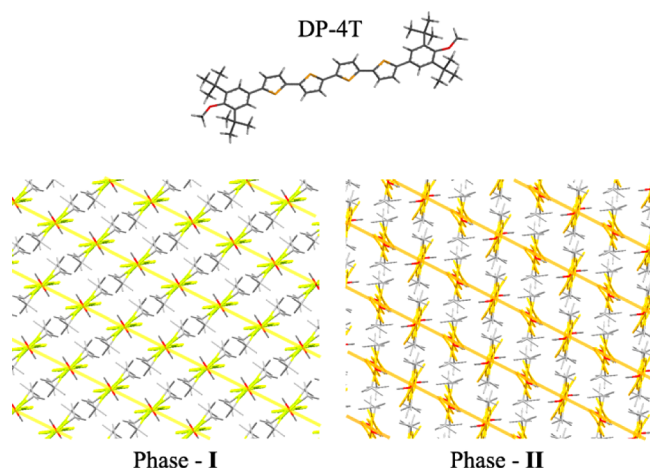


**Figure 1.** Crystal structures of phase-I and phase-II DP-4T shown along the direction of the 4T backbone. Thick yellow and orange lines evidence layers characterized by the most significant interaromatic intermolecular interactions generated by translation along the  $a$ -axis and half of the  $b$  axis, for phase-I and -II, respectively.

specifically, phase-I is formed by standard solution crystallization techniques, whereas the second phase (phase-II) is obtained only by controlled thermal treatment. As the two polymorphs (see Table 1) show different photoluminescence (PL) properties, though with very similar spectral profiles, they provide an ideal case to correlate structural information and quantum chemical (QC) calculations with their different emissive behavior.

From solution, DP-4T (phase-I) crystallizes in space group  $P-1$  with half of a molecule in the asymmetric unit and a single DP-4T molecule in the unit cell (see Table S1 (SI) and Figure 2). The thienylene moiety adopts an all-trans conformation and shows good planarity (rmsd = 0.08 Å), while the terminal phenyl rings form a  $35^\circ$  angle with respect to the mean thienylene plane. In phase-I crystals, molecules arrange parallel in loose stacks (see Figures 1 and 2), deviating from the typical herringbone motif observed in most end-substituted and unsubstituted oligothiophenes. Pitch and roll angles,<sup>21</sup> as defined by Curtis et al. to describe  $\pi$ -stacked structures,

**Table 1. Structural and PL Properties of DP-4T Polymorphs**

	density (Mg m <sup>-3</sup> )	$E_{\text{Subl}}$ (kcal mol <sup>-1</sup> ) <sup>a</sup>	voids (%) <sup>b</sup>	mp (°C)	PL-QY (%)	PL max. (eV)	$k_{\text{rad}}$ (s <sup>-1</sup> ) <sup>c</sup>	exciton splitting <sup>d</sup> (eV)
phase-I	1.202	40.0	3.4	195	18	2.27	$4.7 \times 10^8$	0.22
phase-II	1.196	40.6	0.0	217	11	2.19	$2.2 \times 10^8$	0.29

<sup>a</sup>Obtained from DFT solid-state calculations (details are reported in the text). <sup>b</sup>Voided calculated as a percentage of the unit cell volume with a 1.2 Å probe radius and a 0.2 Å grid spacing on Mercury CSDS (Figure S2, Supporting Information (SI)). <sup>c</sup>Obtained from PL lifetime experiments described later in the text (details in the SI). <sup>d</sup>Obtained from TD-DFT excited-state calculations.

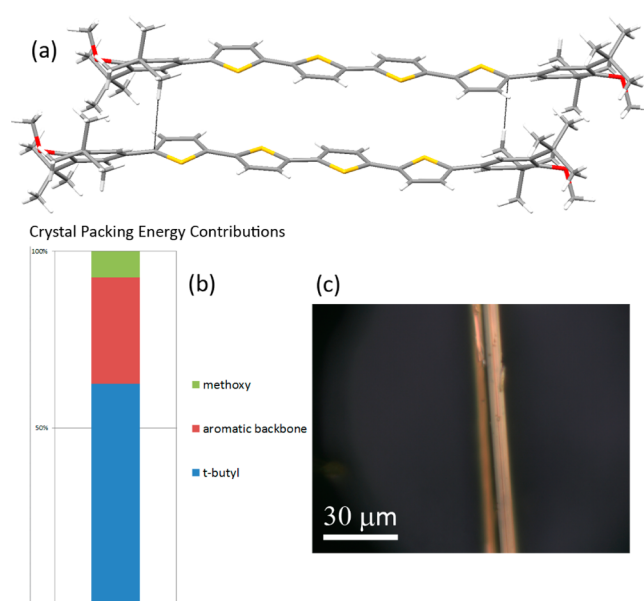


**Figure 2.** Crystal structure of phase-I. (a) View of two DP-4T molecules showing short contacts stemming from alkyl C-H $\cdots\pi$  interactions (shown as black lines). (b) Crystal packing energy contributions of methoxy, aromatic backbone and *tert*-butyl moieties. (c) Needle-like crystal of phase-I.

correspond to  $43$  and  $58^\circ$ , respectively. The steric requirements of *tert*-butyl substituents are plausibly a key factor leading to the phase-I molecular arrangement.

Phase-II crystals may be obtained quantitatively by appropriate thermal treatment of phase-I, while attempts to grow single crystals of phase-II from solution, either by spontaneous nucleation or by seeding methods, were unsuccessful,<sup>22</sup> always resulting in phase-I crystals. Specifically, keeping single crystals of phase-I at  $195^\circ\text{C}$  for 30 min results in the conversion into phase-II orange single crystals of sufficient size ( $>50\ \mu\text{m}$ ) and quality for high-resolution X-ray diffraction. Interestingly, the original needle shape of phase-I crystals (Figures 2c, 3c, and S3 (SI) in situ optical micrographs) is retained also by polycrystalline phase-II material.

The space group of phase-II is also  $P-1$ , but the asymmetric unit is now defined by two independent half molecules (Table S1 (SI) and Figure 3a), and hence, two different molecules are present in the unit cell. Because the midpoint of both molecules lies on crystallographic centers of inversion, the central interthiophene bond is trans in both DP-4T molecules. In one case, the tetrathiophene ring system is arranged in a cis-trans-cis planar conformation (out-of-plane rmsd = 0.06 Å), while the second molecule in phase-II retains the all-trans conformation found in phase-I, however with a more pronounced distortion from planarity (rmsd = 0.19 Å). The phenyl rings in both phase-II conformers remain tilted at about  $30^\circ$  from the plane of the adjacent thiophenes. A further

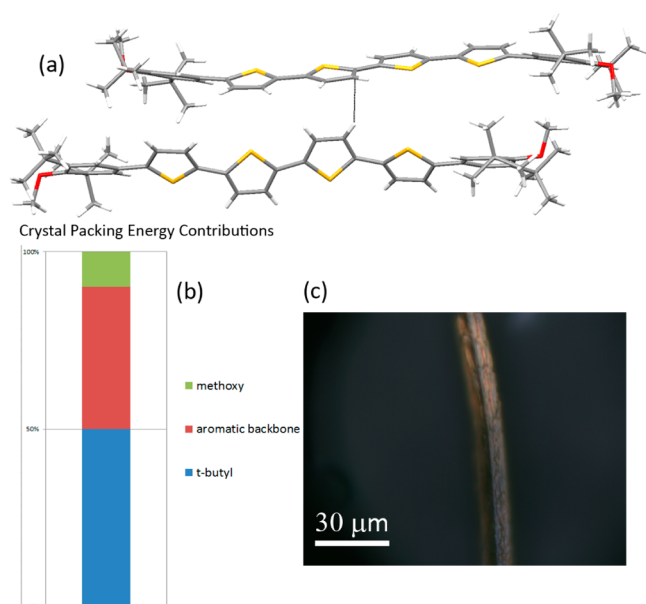


**Figure 3.** Crystal structure of phase-II. (a) View of two DP-4T molecules showing short contacts stemming from aromatic C–H $\cdots\pi$  interactions (shown as black lines). (b) Crystal packing energy contributions of methoxy, aromatic backbone and *tert*-butyl moieties. (c) Crystal of phase-I after transformation to phase-II polycrystalline aggregate.

relevant feature of the phase-II structure is the loss of the parallel stacking arrangement observed in phase-I as the two independent molecules form a T-shaped dimer in which the *cis*–*trans*–*cis* conformer faces edge-on to the all-*trans* molecule at an angle of 71°. The arrangement of the DP-4T molecules in phase-II is thus a herringbone-like packing (Figure 3a) and not the parallel stacking found in phase-I. The slightly denser (+0.5%) phase-I with optimized bulky side group packing allows for relatively large voids between loosely packed central tetrathiphene units (Figure S2, SI). There are no such voids in phase-II, which presents a lower density and a much higher melting point (Table 1).

In order to make sense of the apparently conflicting structural, thermal, and emissive properties of the two polymorphs, the packing of DP-4T molecules in both polymorphs has been analyzed by solid-state density functional theory (DFT) methods under periodical boundary conditions. In particular the Perdew–Wang (PWC) functional<sup>23</sup> coupled with a double- $\zeta$  quality basis set including polarization functions on all atoms (i.e., DNP) was used as implemented in the DMol<sup>3</sup> software.<sup>24</sup> The same level of calculation employed here proved to be adequate for large supramolecular systems,<sup>25–28</sup> charged-particle-containing systems,<sup>29–32</sup> and crystalline phases of thiophene-based oligomers and polymers.<sup>33</sup> More specifically, in the latter case, it was shown that calculated heats of sublimation are in good agreement with the experimental values. The analysis performed on the phase-I crystal structure yields a sublimation energy of 40.0 kcal/mol. The relative contributions to the crystal packing energy (see the SI for details) are depicted as a histogram (Figure 2b). A 63% contribution is due to the *tert*-butyl moieties that form C–H $\cdots\pi$  interactions between neighboring molecules along the stacking direction. DFT calculations suggest a slightly higher sublimation energy ( $\Delta E_{\text{II-I}} \approx +0.6$  kcal/mol) for the higher melting polymorph phase-II consistent with calorimetric data

(see the SI). *Tert*-butyl groups still majorly contribute to crystal packing but do not appear to be involved in any type of specific stabilizing interactions; this might explain the large thermal parameters found for the atoms of these substituents, likely characterized by substantial conformational freedom within the crystal lattice. The packing energy of phase-II involves comparable contributions of the aromatic backbone and *tert*-butyl groups, 50% and 40%, respectively. This is consistent with the loss of alkyl C–H $\cdots\pi$  interactions and the development of aromatic C–H $\cdots\pi$  interactions between  $\beta$ -hydrogens of thiophene moieties in phase-II, evidenced by the short contacts in the crystal structure (Figure 3a). The evidenced difference in interaromatic interactions found in the two phases may well be a key to understand differences in optical properties of the polymorphs of this conjugated backbone material.

PL spectra of the two DP-4T single-crystal polymorphs (Figure 4) show well-resolved vibronic progressions closely

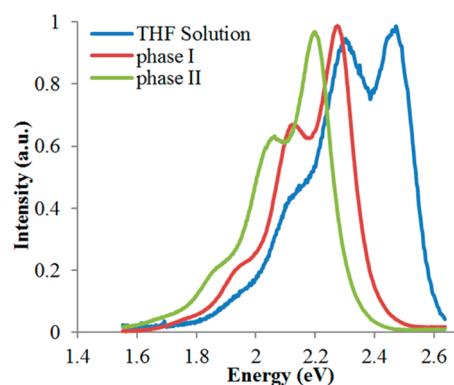


**Figure 4.** PL spectra ( $\lambda_{\text{exc}} = 420$  nm) of DP-4T in phase-I and phase-II crystals and in THF solution. Excitation profiles are given in Figure S5 (SI).

resembling that observed for this thiophene–phenylene hexamer derivative in solution, although with two noticeable differences: (i) the relative intensities of the vibronic replica change from the solution to the two solid-state phases, as expected in the case of H-like aggregation; (ii) an increasing emission red-shift is detected as we move from solution to phase-I and to phase-II.

PL QYs of phase-I and -II are, respectively, 18% and 11%, not too far from the 56% measured in solution. Emission lifetime measurements give us further insight about the dynamics of the excited states of DP-4T in the solid state and, in particular, into mechanisms determining the crystal emission efficiencies. For phase-I, the QY/emission lifetime data yield  $k_{\text{rad}} = 4.7 \times 10^8 \text{ s}^{-1}$  ( $k_{\text{rad}}$  can be calculated as the ratio between the PL-QY and the total decay time [ $k_{\text{rad}} = \text{QY}/\tau_{\text{tot}}$ ]), only slightly smaller than that of the same molecules in solution, which is  $7.2 \times 10^8 \text{ s}^{-1}$ . On the contrary, in phase-II, a low QY is associated with a long PL lifetime and hence results in an unrealistically small  $k_{\text{rad}} = 2.2 \times 10^8 \text{ s}^{-1}$  (see the SI for time-resolved data and  $k_{\text{rad}}$  calculation details), which can be considered nothing more than a rough lower boundary for the phase-II radiative constant. This discrepancy cannot be explained only by a reabsorption effect, which is expected to be similar for the analyzed crystals of comparable size (10–50  $\mu\text{m}$ ). Conversely, the simultaneous occurrence of a low QY and a long-lived emission suggests that the particular packing of this structure may induce the formation of dark states that gather a

fraction of the excitation, reducing the number of available emitting excited states.

In order to further detail the picture of allowed electronic transitions of DP-4T in both phases, single excitations and the corresponding transition dipole moments (TDMs) need to be evaluated. TDMs for oligothiophenes stacked in a parallel fashion are expected to lie along the aromatic backbone, implying H-like behavior, with side-by-side arrangement of the TDMs.<sup>34</sup> Indeed, 1D clusters of molecules along the closest interaromatic intermolecular interaction direction (see Figures 1 and 5) clearly show H-like mutual arrangements of the

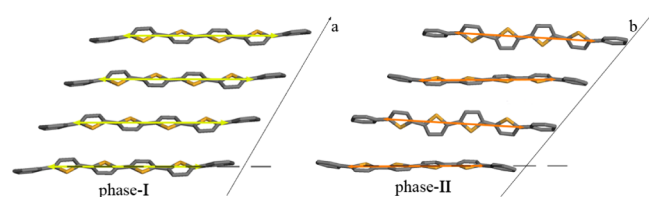


**Figure 5.** 1D clusters of closest neighboring molecules of phase-I (along the *a* axis) and phase-II (along the *b* axis), with superimposed yellow and orange arrows representing calculated TDMs, arranged in parallel stacks, a feature of ideal H-aggregate model.

molecular long axes for both DP-4T phases. Only slight deviations are found for phase-II, which shows some misorientation due to the presence of two independent molecules in the unit cell. Therefore, molecular stacks and expected TDM vectors can both be regarded as H-aggregates; yet, it is the phase closer to the ideal H-model (the angle between the aromatic plane and the stacking axis is closer to 90° for phase-I) that shows the highest QY.

To confirm the previous qualitative considerations, calculations of dimer excited states and TDMs have been carried out by using the semiempirical ZINDO and time-dependent DFT calculations (TD-DFT) methods, which are known to provide reasonable results for the excited states of conjugated molecules.<sup>35–37</sup> The input geometries were first optimized as isolated molecules and then arranged in dimers conforming to crystal packing, that is, preserving the relative positions and orientations. The B3LYP functional was adopted together with a 6-31G\*\* basis set as implemented in the suite of programs GAUSSIAN09,<sup>38</sup> used for all calculations (see details and results in the SI). Calculated TDM vectors, associated with the lowest allowed energy excitations, lie (see Table S2, SI) within the thiophene plane, with small deviations from the main axis for all molecules of both polymorphs. To a first approximation, that is, considering only dimeric interactions and neglecting non-nearest-neighbor interactions, the effect of packing on the couplings among TDM vectors in phase-I and phase-II is very similar, as expected from qualitative considerations, and results in parallel side-by-side arrangement, following H-aggregate absorption selection rules.

One interesting difference resulting from the TD-DFT calculations is that more optical transitions are allowed for phase-II, including the prohibited  $S_0$ – $S_1$  transition, albeit with very low oscillator strength. This result reflects the misorientation of independent molecules present in the unit cell of phase-II, as reported in the previous qualitative geometrical considerations. Moreover, exciton splittings are 0.22 and 0.29 eV for phase-I and phase-II, respectively, implying weaker H-aggregation for phase-I, therefore in agreement with the small reduction of  $k_{\text{rad}}$  found for phase-I

with respect to the DP-4T solution. Dimer excited-state calculations reproduce also quite well the red-shifted emission of both polymorphs with calculated purely electronic excitation energies  $S_1$  of 2.36 and 2.30 eV for phase-I and phase-II, respectively (to be compared with the experimental PL maxima of 2.27 and 2.19 eV), corresponding to a theoretical shift  $\Delta(\text{Gap}_{\text{II}} - \text{Gap}_{\text{I}}) = -0.06$  eV against the observed  $\Delta(\text{PL}_{\text{maxII}} - \text{PL}_{\text{maxI}}) = -0.08$  eV (see the SI). Overall, TD-DFT results are consistent with the hypothesis that the drop of the PL intensity in phase-II DP-4T must be explained by other properties, among which, as suggested above, is the formation of dark charge-transfer states. Further support to this hypothesis stems from the peculiar nature of the phase-II HOMO and LUMO described below. The effect of molecular conformations and dimeric intermolecular interactions on the optical properties of two polymorphs can at least be partly explained by referring to the spatial distribution of their HOMO and LUMO. The phase-II dimer HOMO can be visualized as residing on the all-trans molecule, while the LUMO lies on the cis–trans–cis conformer (see Figure 6). This result suggests that in phase-II, the primary

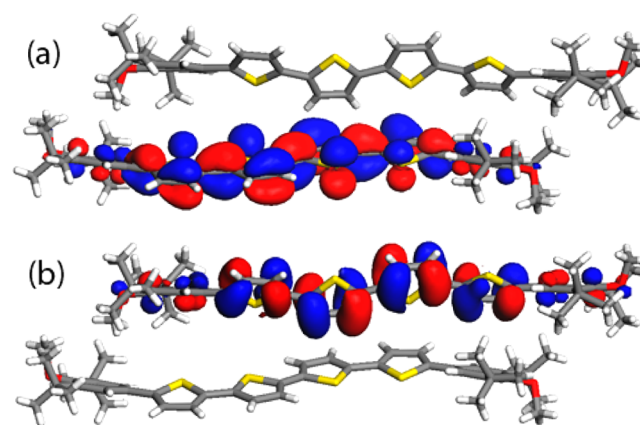


**Figure 6.** LUMO (a) and HOMO (b) orbitals for phase-II DP-4T dimer.

photoexcitation should produce not only Frenkel excitons with a partial charge-transfer character but possibly also dark charge-transfer states with a consequential reduction of the emission QY not related to the presence of defects or excitation traps, as already reported for sexithiophene crystals.<sup>39</sup>

In conclusion, we presented a centrosymmetric end-substituted thiophene–phenylene hexamer that shows an unusual structural polymorphism involving two stable crystal forms that can be selectively obtained. The results of solid-state DFT calculations, coupled with crystallographic data, not only confirm the relative thermal stability of the two polymorphs but also help to understand and quantify intermolecular interactions between aromatic thienylene moieties. The *tert*-butyl groups act as spacers, preventing effective interaromatic interactions between neighboring molecules and allowing for relatively high PL especially in phase-I, which shows marginally higher mass density than phase-II. The contributions to the crystal packing of *tert*-butyl substituents through C–H $\cdots$  $\pi$  interactions effectively lock the relative position of molecules in phase-I to relatively high temperatures. Conversely, the two different backbone conformations of DP-4T in phase-II allow for a tighter interaromatic packing, preventing the formation of the voids found in phase-I around aromatic moieties. In this way, the aromatic components of the molecules interact more

strongly, favoring the formation of dark charge-transfer states and causing a drop in PL efficiency. Also, TD-DFT calculations revealed a different orbital and energy picture of excited states for each structure due to different degrees of coupling between first-neighbor molecules. The polymorphic behavior presented herein affords reasonable insight into the optical properties of the DP-4T system, likely offering generally applicable guidelines. It confirms that solid-state optical spectral properties of a given molecular species, even in the presence of different stable conformers, are likely to vary modestly with packing. On the other hand, neither the bulkiness of substituents, nor H- versus J-aggregate features, nor a generic packing tightness correlating with density or packing energy allows a detailed prediction or modulation of luminescence in the solid state of aromatic oligomers. Control of intermolecular interactions among the aromatic components in aggregates is very likely to be essential. Such features may be quantified by appropriate partitioning of crystal sublimation enthalpies or, more qualitatively, evaluating voids between the aromatic segments of oligomers. In this regard, the presence of sterically demanding nonaromatic side groups must thus be coupled with a stringent control over crystallization conditions in order to obtain optimal molecular packing of the aromatic backbone.

## ASSOCIATED CONTENT

### Supporting Information

Experimental methods, complete crystallographic data, synthetic details, DSC curves, excitation profiles, and theoretical calculations details. This material is available free of charge via the Internet at <http://pubs.acs.org>.

## AUTHOR INFORMATION

### Corresponding Authors

\*E-mail: chiara.bertarelli@polimi.it (C. Bertarelli).

\*E-mail: valdo.meille@polimi.it (S.V. Meille).

### Notes

The authors declare no competing financial interest.

## ACKNOWLEDGMENTS

The authors wish to acknowledge and thank the referees (especially referee 1) for helpful suggestions and comments that allowed a significant improvement of the manuscript. E.P. acknowledges the European Union for financial support (Marie Curie FP7 IRG grant). Fondazione Cariplo is acknowledged for financial support through the InDIXi project grant n. 2011-0368 and the project "PLENOS" (ref 2011-0349). The authors also acknowledge the CINECA and the Lombardia award under the LISA Initiative for the availability of high-performance computing resources and support.

## REFERENCES

- (1) Ichikawa, M.; Hibino, R.; Inoue, M.; Haritani, T.; Hotta, S.; Koyama, T.; Taniguchi, Y. Improved Crystal-Growth and Emission Gain-Narrowing of Thiophene/Phenylene Co-Oligomers. *Adv. Mater.* **2003**, *15*, 213–217.
- (2) Hotta, S.; Yamao, T. The Thiophene/Phenylene Co-Oligomers: Exotic Molecular Semiconductors Integrating High-Performance Electronic and Optical Functionalities. *J. Mater. Chem.* **2011**, *21*, 1295–1304.
- (3) Tavazzi, S.; Miozzo, L.; Silvestri, L.; Mora, S.; Spearman, P.; Moret, M.; Rizzato, S.; Braga, D.; Diaw, A. K. D.; Gningue-Sall, D.; Aaron, J.-J.; Yassar, A. Crystal Structure and Optical Properties of N-Pyrrole End-Capped Thiophene/Phenyl Co-Oligomer: Strong H-

Type Excitonic Coupling and Emission Self-Waveguiding. *Cryst. Growth Des.* **2010**, *10*, 2342–2349.

(4) Fang, H. H.; Ding, R.; Lu, S. Y.; Yang, J.; Zhang, X.-L.; Yang, R.; Feng, J.; Chen, Q.-D.; Song, J.-F.; Sun, H. B. Distributed Feedback Lasers Based on Thiophene/Phenylene Co-Oligomer Single Crystals. *Adv. Funct. Mater.* **2012**, *22*, 33–38.

(5) Tian, H.; Wang, J.; Shi, J.; Yan, D.; Wang, L.; Geng, Y.; Wang, F. Novel Thiophene-Aryl Co-Oligomers for Organic Thin Film Transistors. *J. Mater. Chem.* **2005**, *15*, 3026–3033.

(6) Spano, J. C. Excitons in Conjugated Oligomer Aggregates, Films, and Crystals. *Annu. Rev. Phys. Chem.* **2006**, *57*, 217–243.

(7) Kasha, M.; Rawls, H. R.; Ashraf El-Bayoumi, M. The Exciton Model in Molecular Spectroscopy. *Pure Appl. Chem.* **1965**, *11*, 371–392.

(8) Zhao, Z.; Spano, F. C. Multiple Mode Exciton-Phonon Coupling: Applications to Photoluminescence in Oligothiophene Thin Films. *J. Phys. Chem. C* **2007**, *111*, 6113–6123.

(9) Bando, K.; Nakamura, T.; Shimoi, Y.; Kobayashi, S.; Fujiwara, S.; Masumoto, Y.; Sasaki, F.; Hotta, S. Optical Selection Rule for the Lower Davydov Excitons in Co-Oligomer Single Crystals. *Phys. Rev. B* **2008**, *77*, 45205/1–45205/6.

(10) Nakanotani, H.; Adachi, C. Amplified Spontaneous Emission and Electroluminescence from Thiophene/Phenylene Co-Oligomer-Doped *p*-Bis(*p*-styrylstyryl)benzene Crystals. *Adv. Opt. Mater.* **2013**, *1*, 422–427.

(11) Mizuno, H.; Haku, U.; Marutani, Y.; Ishizumi, A.; Yanagi, H.; Sasaki, F.; Hotta, S. Single Crystals of 5,5'-Bis(4'-methoxybiphenyl-4-yl)-2,2'-bithiophene for Organic Laser Media. *Adv. Mater.* **2012**, *24*, 5744–5749.

(12) Yanagi, H.; Morikawa, T.; Hotta, S.; Yase, K. Epitaxial Growth of Thiophene/*p*-Phenylene Co-oligomers for Highly Polarized Light-Emitting Crystals. *Adv. Mater.* **2001**, *13*, 313–317.

(13) Bando, K.; Nakamura, T.; Kobayashi, S.; Masumoto, Y.; Sasaki, F.; Hotta, S. Origin of the Amplified Spontaneous Emission from Thiophene/Phenylene Co-Oligomer Single Crystals: Towards Co-Oligomer Lasers. *J. Appl. Phys.* **2006**, *99*, 13518/1–13518/6.

(14) Meinardi, F.; Blumstengel, S.; Cerminara, M.; Macchi, G.; Tubino, R. Intrinsic Excitonic Luminescence in Crystalline Terthiophene. *Phys. Rev. B* **2005**, *72*, 35207.

(15) Gierschner, J.; Park, S. Y. Luminescent Distyrylbenzenes: Tailoring Molecular Structure and Crystalline Morphology. *J. Mater. Chem. C* **2013**, *1*, 5818–5832.

(16) Nishinaga, T.; Wakamiya, A.; Yamazaki, D.; Komatsu, K. Crystal Structures and Spectroscopic Characterization of Radical Cations and Dications of Oligothiophenes Stabilized by Annulation with Bicyclo[2.2.2]octene Units: Sterically Segregated Cationic Oligothiophenes. *J. Am. Chem. Soc.* **2004**, *126*, 3163–3174.

(17) Varghese, S.; Park, S. K.; Casado, S.; Fischer, R. C.; Resel, R.; Milián-Medina, B.; Wannemacher, R.; Park, S. Y.; Gierschner, J. Stimulated Emission Properties of Sterically Modified Distyrylbenzene-Based H-Aggregate Single Crystals. *J. Phys. Chem. Lett.* **2013**, *4*, 1597–1602.

(18) Fichou, D. Structural Order in Conjugated Oligothiophenes and Its Implications on Opto-Electronic Devices. *J. Mater. Chem.* **2000**, *10*, 571–588.

(19) Barbarella, G.; Zambianchi, M.; Del Fresno, I.; Marimon, M.; Antolini, L.; Bongini, A. Conformational Polymorphism of Oligothiophenes: X-Ray Structure of the Monoclinic Form of 3,3,4,3-Tetrakis(methylsulfanyl)-2,2':5',2'':5'',2'''-Quaterthiophene. *Adv. Mater.* **1997**, *9*, 484–487.

(20) Canesi, E. V.; Dassa, G.; Botta, C.; Bianco, A.; Bertarelli, C.; Zerbi, G. Optical Features of Substituted Phenyl End-Capped Oligothiophenes. *Open Chem. Phys. J.* **2008**, *1*, 23–28.

(21) Curtis, M. D.; Cao, J.; Kampf, J. W. Solid-State Packing of Conjugated Oligomers: From  $\pi$ -Stacks to the Herringbone Structure. *J. Am. Chem. Soc.* **2004**, *126*, 4318–4328.

(22) Dunitz, J. D.; Bernstein, J. Disappearing Polymorphs. *Acc. Chem. Res.* **1995**, *28*, 193–200.

- (23) Perdew, J. P.; Wang, Y. Accurate and Simple Analytic Representation of the Electron–Gas Correlation Energy. *Phys. Rev. B* **1992**, *45*, 13244–13249.
- (24) Delley, B. From Molecules to Solids with the DMol3 Approach. *J. Chem. Phys.* **2000**, *113*, 7756–7761.
- (25) Kolokoltsev, Y.; Amelines-Sarria, O.; Gromovoy, T. Y.; Basiuk, V. A. Interaction of meso-Tetraphenylporphines with C60 Fullerene: Comparison of Several Density Functional Theory Functionals Implemented in DMol3 Module. *J. Comput. Theor. Nanosci.* **2010**, *7*, 1095–1103.
- (26) Amelines-Sarria, O.; Kolokoltsev, Y.; Basiuk, V. A. Noncovalent 1:2 Complex of meso-Tetraphenylporphine with C60 Fullerene: A Density Functional Theory Study. *J. Comput. Theor. Nanosci.* **2010**, *7*, 1996–2003.
- (27) Basiuk, V. A.; Amelines-Sarria, O.; Kolokoltsev, Y. A Density Functional Theory Study of Porphyrin–Pyridine–Fullerene Triad ZnTPP·Py·C60. *J. Comput. Theor. Nanosci.* **2010**, *7*, 2322–2330.
- (28) Basiuk, V. A. Electron Smearing in DFT Calculations: A Case Study of Doxorubicin Interaction with Single-Walled Carbon Nanotubes. *Int. J. Quantum Chem.* **2011**, *15*, 4197–4205.
- (29) Yu, G.; Yin, S.; Liu, Y.; Shuai, Z.; Zhu, D. Structures, Electronic States, and Electroluminescent Properties of a Zinc(II) 2-(2-Hydroxyphenyl)benzothiazolate Complex. *J. Am. Chem. Soc.* **2003**, *125*, 14816–14824.
- (30) Guo, F.; Zhang, M. Q.; Famulari, A.; Martí-Rujas, J. Solid State Transformations in Stoichiometric Hydrogen Bonded Molecular Salts: Ionic Interconversion and Dehydration Processes. *CrystEngComm* **2013**, *15*, 6237–6243.
- (31) Guo, F.; Shao, H.; Yang, Q.; Famulari, A.; Martí-Rujas, J. Mechanochemical Dehydrochlorination and Chelation Reaction in the Solid State: From a Molecular Salt to a Coordination Complex. *CrystEngComm* **2014**, *16*, 969–973.
- (32) Maccaroni, E.; Malpezzi, L.; Famulari, A.; Masciocchi, N. Structural and Energetic Aspects of a New Bupropion Hydrochloride Polymorph. *J. Pharmaceut. Biomed. Anal.* **2012**, *60*, 65–70.
- (33) Famulari, A.; Raos, G.; Casalegno, M.; Po, R.; Meille, S. V. A Solid State Density Functional Study of Crystalline Thiophene-Based Oligomers and Polymers. *J. Phys. Chem. B* **2012**, *116*, 14504–14509.
- (34) Gierschner, J.; Lüer, L.; Milián-Medina, B.; Oelkrug, D.; Egelhaaf, H.-J. Highly Emissive H-Aggregates or Aggregation-Induced Emission Quenching? The Photophysics of All-Trans *para*-Distyrylbenzene. *J. Phys. Chem. Lett.* **2013**, *4*, 2686–2697.
- (35) Tretiak, S.; Mukamel, S. Density Matrix Analysis and Simulation of Electronic Excitations in Conjugated and Aggregated Molecules. *Chem. Rev.* **2002**, *102*, 3171–3212.
- (36) Ottonelli, M.; Musso, G.; Dellepiane, G. Evolution of the Bipolaronic Structure in Going From One- to Two-Dimensional  $\pi$  Model Systems. *J. Phys. Chem. A* **2008**, *112*, 3991–3995.
- (37) Quarti, C.; Fazzi, D.; Tommasini, M. A Computational Investigation on Singlet and Triplet Exciton Couplings in Acene Molecular Crystals. *Chem. Phys. Lett.* **2010**, *496*, 284–290.
- (38) Frisch, M. J.; Trucks, G. W.; Schlegel, H. B.; Scuseria, G. E.; Robb, M. A.; Cheeseman, J. R.; Scalmani, G.; Barone, V.; Mennucci, B.; Petersson, G. A.; et al. *Gaussian 09*, revision A.1, Gaussian, Inc.: Wallingford, CT, 2009.
- (39) Glowe, J.; Perrin, M.; Beljonne, D.; Hayes, S. C.; Gardebien, F.; Silva, C. Charge-Transfer Excitons in Strongly Coupled Organic Semiconductors. *Phys. Rev. B* **2010**, *81*, 041201(R).